Synoptic Meteorology I: Divergence and Vertical Motion

For Further Reading

The isobaric form of the continuity equation is presented in Section 1.3 of *Midlatitude Synoptic Meteorology* by G. Lackmann, among other references. The evaluation of divergence using integral-based methods is discussed in Section 4-4 of *Weather Analysis* by D. Djurić. The relationship between divergence and vertical motion is discussed in Section 4-5 of *Weather Analysis*. A derivation of the mass continuity equation and its basic application to vertical motion is also provided by Section 4.1 of *Mid-Latitude Atmospheric Dynamics* by J. Martin.

Why Do We Care About Vertical Motion?

We care about vertical motion for several reasons…

- Condensation, and thus cloud and precipitation formation, generally occurs from cooling an air parcel (or layer) to saturation through ascent.
- As we will demonstrate next semester, mid-latitude cyclone and anticyclone formation, decay, and movement are functions of patterns of ascent and descent.
- Vertical vorticity amplification and generation are related to vertical motion and its horizontal gradients.

One might ask, how do we evaluate vertical motion, whether qualitatively or quantitatively? In this lecture, we consider one method of doing so, by relating vertical motion to divergence. We will explore other methods for doing so in greater detail next semester.

Divergence Calculation Methods

In our previous lecture, we defined divergence as:

$$\delta = \frac{\partial u}{\partial x} + \frac{\partial v}{\partial y} \tag{1a}$$

$$\delta = \frac{\partial V}{\partial s} - V\frac{\partial \alpha}{\partial n} \tag{1b}$$

where (1a) is divergence represented in Cartesian coordinates and (1b) is divergence represented in natural coordinates. Given at least four wind observations – two each along the *x*- and *y*- or *s*- and *n*-axes – one can use centered finite difference approximations to compute divergence. This is illustrated in a Cartesian coordinate system in Figure 1.

The process of evaluating divergence in this way can be cumbersome, however, because of the need to first convert each wind observation to its *u* and *v* components. Evaluating divergence using

natural coordinates can help overcome this hurdle but is best for qualitative rather than quantitative purposes. Furthermore, because we rarely have observations over a uniform grid as in Figure 1, we often have to interpolate data onto such a grid to calculate divergence using finite differences. Finally, recall that finite differences are approximations by their very nature and are formally valid only over finite distances (here, ∂x and ∂y). It is up to the analyst to determine whether these limitations are acceptable or not for the case being considered.

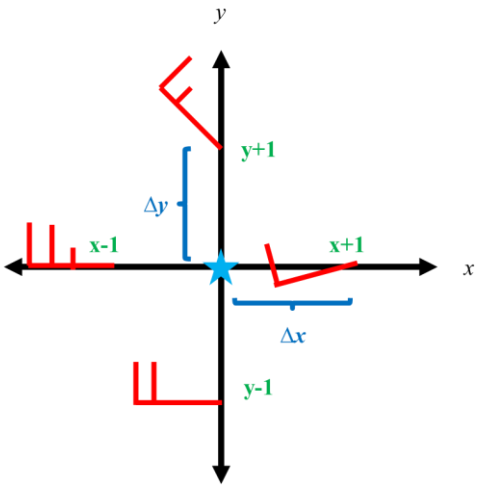

Figure 1. Conceptual example of evaluating divergence at the location given by the blue star using a centered finite difference and winds (half-flag: 5 kt, flag: 10 kt, pennant: 50 kt) from four surrounding observing locations, located at points *x-1*, *x+1*, *y-1*, and *y+1*. The distances Δx and Δy are indicated by the blue text and brackets and, formally, are in meters.

Alternatively, one could use an integral-based method to calculate the divergence into or out of any desired area. For any arbitrary two-dimensional region, the divergence within that region is defined (from calculus) as:

$$\delta = \frac{1}{A}\lim_{A\to 0}\iint_A \nabla\cdot\vec{v}\,da \tag{2}$$

In (2), *A* denotes the area of the two-dimensional region, and the double integral represents integration about the region with area *A*. Omitting the limit, (2) can be approximated as:

$$\delta \approx \overline{\nabla\cdot\vec{v}} = \frac{1}{A}\iint_A \nabla\cdot\vec{v}\,da \tag{3}$$

The overbar in (3) indicates a quantity that is averaged over the area A of the region. If we apply Green's theorem to (3), we obtain:

$$\delta = \frac{1}{A}\int_L v_n dl \tag{4}$$

In (4), L represents the boundary of the region with area A, dl represents a finite line segment along L, and v_n represents the component of the wind normal (perpendicular) to L (where $v_n > 0$ for outward-directed flow and $v_n < 0$ for inward-directed flow).

Approximating the integral in (4) with a summation, we obtain:

$$\delta \approx \frac{1}{A}\sum_{l \to L} v_n \Delta l \tag{5}$$

Equation (5) states that if we know the component of the wind normal to our region at a number of different locations along L, the distance Δl between locations along L, and the area A of the region cut out by L, we can compute the mean divergence within the region. This calculation works best when many observations – such as obtained from a model grid – are available. A conceptual example of how this may be done qualitatively is presented in Figure 2.

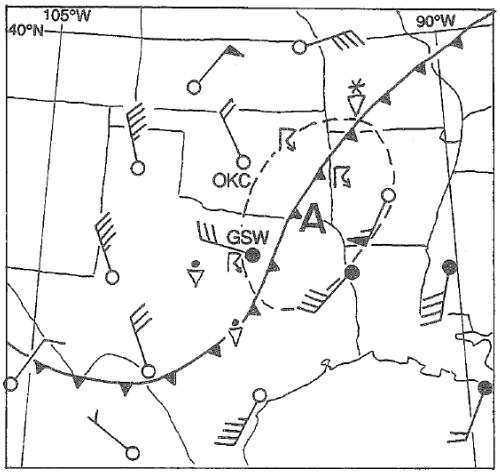

Figure 2. 850 hPa wind (barbs; half-flag: 5 kt, flag: 10 kt, pennant: 50 kt), surface frontal boundary locations (solid triangled line), and sensible weather (symbols) at 0000 UTC 27 January 1969. The dashed region surrounding location **A** is the region considered in the discussion below. Figure reproduced from *Weather Analysis* by D. Djurić, their Figure 4-8.

Consider the portion of the dashed region located east of the surface cold front. We have two wind observations, both roughly aligned parallel to the dashed line. The normal component of the wind

at these locations, then, is zero. Given that the observations imply that the 850 hPa is out of the southwest at 40-55 kt across this entire area, there is a large inward-directed normal component of the wind on the southern edge of the dotted region. This is balanced by a large outward-directed normal component of the wind on the north-northeastern flank of the dotted region, however.

Now consider the portion of the dashed region located to the west of the surface cold front. We have two wind observations, both roughly aligned normal to the dashed line. As both are directed inward, we have a negative contribution to our summation in (5). We can infer from the wind observation in northeastern Kansas that the wind is likely roughly parallel to the dotted region on its far northern extent. Thus, summing all contributions, we assess that the mean divergence in the dotted region is negative, implying convergence. We could also explicitly calculate this using (5) by interpolating the wind observations to the dotted line, computing the normal component of the wind at each location, and determining the distance along the dotted line between each observation.

There do exist other methods of computing divergence, such as the Bellamy method for computing divergence at a location given wind observations at three nearby locations. As a result, the above is not intended to be a comprehensive listing of how divergence may be calculated. It is sufficient for our purposes, however, and enables us to move forward to relating divergence and vertical motion.

The Relationship Between Divergence and Vertical Motion

The continuity equation, expressed in isobaric coordinates, is given by:

$$\frac{\partial u}{\partial x} + \frac{\partial v}{\partial y} + \frac{\partial \omega}{\partial p} = 0 \tag{6}$$

Equation (6) states that atmospheric mass is conserved. For our purposes, we will proceed as though this is always the case. However, interested readers should consult Section 1.3 of *Midlatitude Synoptic Meteorology* by G. Lackmann for a discussion of exceptions to this rule.

The first two terms on the left-hand side of (6) should be familiar to us by now: they represent the horizontal divergence on an isobaric surface. If we rewrite (6) with this, we obtain:

$$\delta = -\frac{\partial \omega}{\partial p} \tag{7}$$

Note that we have moved the remaining partial derivative term to the right-hand side of the equation. Equation (7) states that a given location, the negative of the partial derivative of vertical motion ω with respect to pressure p is equal to the divergence. Stated differently, (7) indicates that the divergence on an isobaric surface is related to how vertical velocity changes with height.

Let us now integrate (7) between two arbitrary isobaric surfaces p_b and p_t, where $p_b > p_t$ (i.e., p_b is found closer to the surface than is p_t given that pressure decreases with increasing altitude). If we do so, we obtain:

$$\int_{p_b}^{p_t} \delta dp = -\int_{p_b}^{p_t} \frac{\partial \omega}{\partial p} dp \tag{8}$$

The right-hand side of (8) can be approximated as $-\int_{p_b}^{p_t} \partial\omega$, which is equal to $-(\omega(p_t) - \omega(p_b))$. If we substitute this in to (8), we obtain:

$$\int_{p_b}^{p_t} \delta dp = -\left(\omega(p_t) - \omega(p_b)\right) \tag{9}$$

Equation (9) makes clear the relationship between divergence and vertical motion. Specifically, the difference in vertical motion ω over some vertical layer bounded by two isobaric levels p_b and p_t (where $p_b > p_t$) is equal to the vertically integrated divergence within that layer.

We can continue to operate on (9) if we desire. If we replace δ by $\overline{\delta}$, the pressure-weighted average divergence within the layer between p_b and p_t, then the left-hand side of (9) can be approximated as $\overline{\delta}\int_{p_b}^{p_t} dp$, which is equal to $\overline{\delta}[p_t - p_b]$. Substituting, we obtain:

$$\overline{\delta}[p_b - p_t] = \omega(p_t) - \omega(p_b) \tag{10}$$

Note that we have moved the leading negative from the right-hand side to the left-hand side of the equation, allowing us to flip the order of the subtraction. Equation (10) states that the difference in vertical motion over a vertical layer bounded by p_t and p_b is directly related to the layer-mean divergence in the vertical layer.

In this discussion, we have attributed the divergence to the divergence of the total wind. However, recall that to good approximation, we stated that the geostrophic wind is non-divergent. Thus, the divergence in this discussion can be viewed as equal to the divergence of the ageostrophic wind.

Dines' Compensation and the Level of Non-Divergence

Derivation

Let us now consider a hypothetical atmosphere comprised of two layers: one between the surface (p_{sfc}) and some middle tropospheric isobaric level (p_L), and one between some middle tropospheric isobaric level (p_L) and the tropopause (p_{trop}). This is depicted in Figure 3 below.

Figure 3. Hypothetical atmosphere comprised of two layers, as described in the text above.

Let us apply (9) for each of these two layers. For the lower layer, where $p_b = p_{sfc}$ and $p_t = p_L$, we obtain:

$$\int_{p_{sfc}}^{p_L} \delta dp = -\left(\omega\left(p_L\right) - \omega\left(p_{sfc}\right)\right) \tag{11a}$$

The surface is a rigid bound on vertical motions; right at the surface, ω is equal to zero. Thus, $\omega(p_{sfc}) = 0$, such that (11a) simplifies to:

$$-\int_{p_{sfc}}^{p_L} \delta dp = \omega\left(p_L\right) \tag{11b}$$

For the upper layer, where $p_b = p_L$ and $p_t = p_{trop}$, we obtain:

$$\int_{p_L}^{p_{trop}} \delta dp = -\left(\omega\left(p_{trop}\right) - \omega\left(p_L\right)\right) \tag{12a}$$

Due to the large atmospheric stability found at the tropopause, the tropopause itself is also treated as a rigid bound on vertical motion; at the tropopause, outside of intense small-scale ascent such as in thunderstorms, ω is equal to zero. Thus, $\omega(p_{trop}) = 0$, such that (12a) simplifies to:

$$\int_{p_L}^{p_{trop}} \delta dp = \omega(p_L) \tag{12b}$$

Upon inspection, we have two separate equations for $\omega(p_L)$, as given by (11b) and (12b). If we equate these equations, we obtain:

$$-\int_{p_{sfc}}^{p_L} \delta dp = \int_{p_L}^{p_{trop}} \delta dp \tag{13}$$

In other words, *the vertically integrated divergence in the lower layer is cancelled out by the vertically integrated divergence in the upper layer*. Stated differently, the divergence within the lower layer is equal in magnitude and opposite in sign to the divergence in the upper layer. This implies that the two are in balance with each other, such that one compensates for the other. This important principle is known as *Dines' compensation principle*.

The sign of divergence must change at least once between p_{sfc} and p_{trop} for (13) to be true. Thus, an important corollary to Dines' compensation principle states that *there must be at least one level at which the divergence is zero*. This level is the *level of non-divergence*. In the troposphere, we often find a level of non-divergence in the middle troposphere, typically between 500-600 hPa. This is why (in part, at least) either of these standard isobaric levels are typically understood to be the *steering level* for synoptic-scale mid-latitude weather systems.

Application

Let us consider a couple of examples. First, consider the case where there is convergence in the lower layer. From Dines' compensation principle, this must be balanced by divergence in the upper layer. There must be a level of non-divergence at the interface between the two layers, or at p_L. We can use this information to obtain the sign of ω at p_L. Given $\delta < 0$ within the lower layer, $p_L < p_{sfc}$, and a leading negative sign on the entire expression, we know that the left-hand side of (11b) – and thus $\omega(p_L)$ – is negative. This indicates ascent at p_L. Likewise, given $\delta > 0$ in the upper layer and $p_{trop} < p_L$, the right-hand side of (12b) – and thus $\omega(p_L)$ again – is negative. This provides a sanity check on our solution. Vertical profiles of divergence and vertical motion accompanying this example are provided in Figure 4.

Next, consider the case of divergence in the lower layer. From Dines' compensation principle, this must be balanced by convergence in the upper layer. There must be a level of non-divergence at the interface between the two layers, or at p_L. We can use this information to obtain the sign of ω at p_L. Given $\delta > 0$ in the lower layer, $p_L < p_{sfc}$, and a leading negative sign on the entire expression, the left-hand side of (11b) – and thus $\omega(p_L)$ – is positive. This indicates descent at p_L. Likewise, given $\delta < 0$ in the upper layer and $p_{trop} < p_L$, the right-hand side of (12b) – and thus $\omega(p_L)$ again –

is positive. Profiles of divergence and vertical motion accompanying this example are provided in Figure 5.

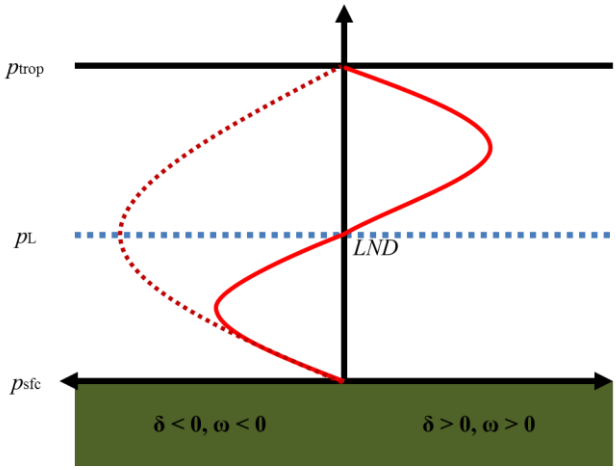

Figure 4. Vertical profiles of divergence (solid red line) and vertical motion (dashed red line) corresponding to the case of convergence in the lower layer, divergence in the upper layer, and the level of non-divergence at the interface between the two layers. Note how ascent ($\omega < 0$) is maximized at the level of non-divergence (*LND*).

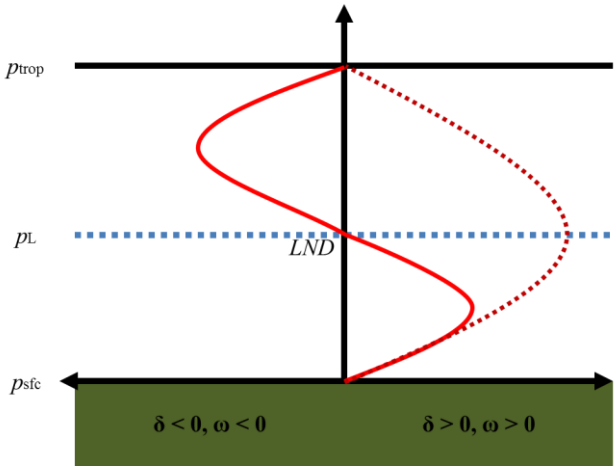

Figure 5. Vertical profiles of divergence (solid red line) and vertical motion (dashed red line) corresponding to the case of divergence in the lower layer, convergence in the upper layer, and the level of non-divergence at the interface between the two layers. Note how descent ($\omega > 0$) is maximized at the level of non-divergence (*LND*).

The real atmosphere typically cannot be considered by two vertical layers. However, it is relatively straightforward to evaluate the vertical profile of vertical motion given patterns of divergence even in quite complex situations. Let us start with equation (9), which we repeat below for simplicity:

$$\int_{p_b}^{p_t} \delta dp = -(\omega(p_t) - \omega(p_b))$$

If we let $p_b = p_{sfc}$, then $\omega(p_{sfc}) = 0$. Thus, the above equation becomes:

$$\omega(p_t) = -\int_{p_{sfc}}^{p_t} \delta dp \tag{14}$$

In other words, *the vertical motion at any isobaric level p_t is equal to the negative of the integrated divergence between the surface and p_t*. Thus, given a vertical profile of divergence, we can start at the surface and integrate upward to obtain the corresponding vertical profile of vertical motion. Examples are presented in Figures 6 and 7.

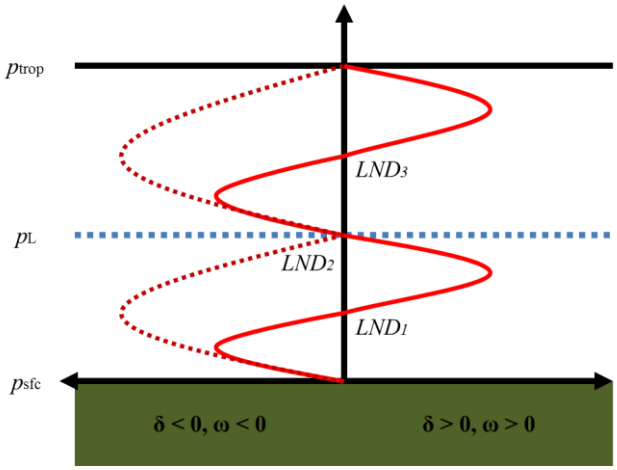

Figure 6. Vertical profiles of divergence (solid red line) and vertical motion (dashed red line) corresponding to the case of equal areas of convergence-divergence-convergence-divergence from the surface to the tropopause. Note how ascent is either maximized or is zero at a level of non-divergence, depending upon the vertical integral of δ from the surface to that altitude.

In Figure 6, we are presented with an example akin to Figure 4. Starting at the surface and working upward, we begin with convergence and, thus, ascent. This makes sense: converging air at ground level must go somewhere, and if it cannot go down into the ground, it must go up.

When the vertical integral of divergence reaches its maximum negative value – where the vertical profile of divergence switches from convergence to divergence, or the first level of non-divergence – ascent is maximized. Ascent decreases to zero when the vertical integral of divergence becomes zero at p_L, whereupon the area of convergence near the surface becomes exactly balanced by the area of divergence above it. The pattern repeats as you continue upward from p_L.

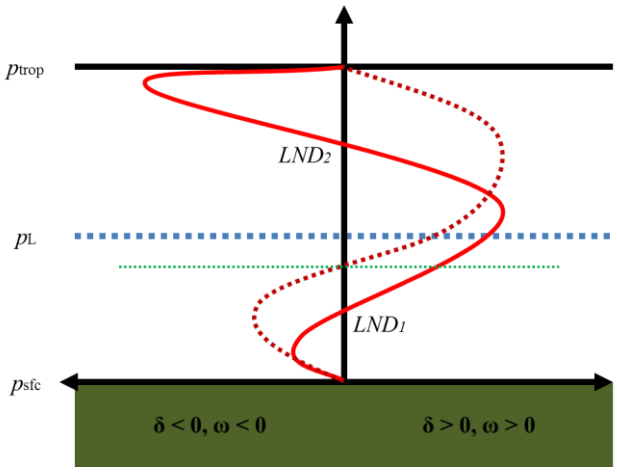

Figure 7. Vertical profiles of divergence (solid red line) and vertical motion (dashed red line) corresponding to the case of unequal areas of convergence-divergence-convergence from the surface to the tropopause. The dashed green line indicates the first altitude above the ground where the vertically integrated divergence is zero; the only other such altitude is p_{trop}.

In Figure 7, we are presented with an even more complex – but also more realistic – example. Just above the surface, we find weak convergence that extends over a shallow vertical layer. Ascent peaks at the lower of the two levels of non-divergence and becomes zero at the dotted green line, where the vertically integrated divergence is zero. Divergence is found in the middle troposphere, and consequently descent over a deep vertical layer develops. This descent is maximized at the second level of non-divergence, where the vertical integral of divergence is at a positive maximum, and then decreases to zero at the tropopause as the vertical integral of divergence approaches zero given the shallow layer of strong convergence just below the tropopause.

Application: Friction, the Wind, and Pressure Systems

In an earlier lecture, we noted that friction acts as a *drag* on the near-surface wind. This reduces the magnitude of the Coriolis force. Thus, whether geostrophic or gradient wind balance holds, air parcels near the surface are directed across the isobars/isohypses from high pressure/height toward low pressure/height. Consequently, air diverges from areas of high pressure/height and converges into areas of low pressure/height near the surface.

Because the vertically integrated divergence must be zero between the surface and the tropopause, there must be divergence above near-surface areas of low pressure/height and convergence above near-surface areas of high pressure/height. Further, there must be ascent atop near-surface areas of low pressure/height and descent atop near-surface areas of high pressure/height. This helps explain why near-surface areas of low pressure/height are often accompanied by unsettled weather (tied to ascent) and near-surface areas of high pressure/height are often accompanied by fair weather (tied to descent).

Application: The Four-Quadrant Jet Model

Having defined divergence and diffluence in the previous lecture and linking divergence to vertical motion earlier in this lecture, we can use our newly acquired insight to obtain further information regarding jet-streak structure.

We first consider an idealized view of an upper-tropospheric jet streak, one that is associated with primarily "straight" flow through the jet itself. This is depicted in Figure 8. We define a jet entrance region as the region where the wind accelerates and a jet exit region as the region where the wind decelerates. Likewise, the "right" and "left" sides of the jet are the sides of the jet with your back to the wind. For a westerly jet streak, the right side is to the south and the left side is to the north.

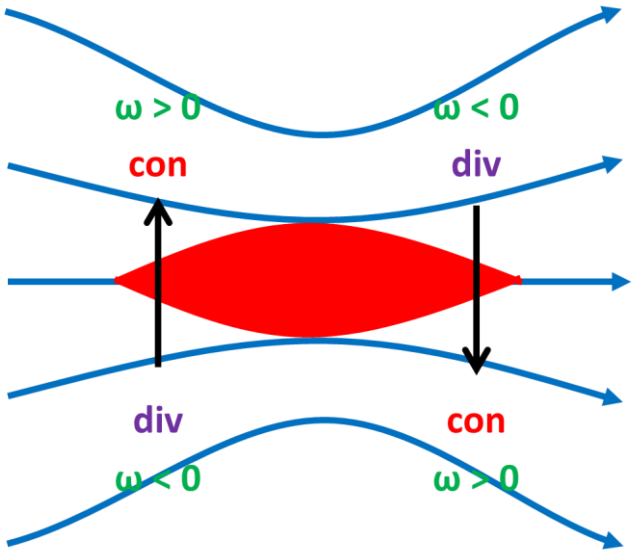

Figure 8. Idealized view of a straight westerly upper-tropospheric jet streak (in red). Hypothetical streamlines are depicted in blue, ageostrophic flow is depicted in black, the resulting convergence and divergence are depicted in red and purple respectively, and pressure vertical velocity (omega; negative values denote ascent) is depicted in green.

When we introduced the concept of the ageostrophic wind earlier this semester, we stated that it could be expressed in terms of parcel accelerations following the flow (in the absence of friction):

$$\frac{Du}{Dt} = fv_{ag} \qquad (15a)$$

$$\frac{Dv}{Dt} = -fu_{ag} \qquad (15b)$$

For the case of the westerly jet streak in Figure 8, it is (1a) that we are most interested in. However, the following analysis can be generalized to a straight jet streak of any orientation.

As a parcel enters the jet, it moves from west to east at a progressively faster rate of speed, meaning that it accelerates in the eastward (or positive *x*-) direction. Thus, following the flow, the left-hand side of (15a) is positive as *u* increases. If we assume that we are in the Northern Hemisphere, such that $f > 0$, v_{ag} is positive, indicating a south-to-north flow across the jet in its entrance region. In the absence of ageostrophic flow elsewhere, this implies divergence in the right entrance region and convergence in the left entrance region. From Dines' compensation principle, the divergence in the right entrance region must be balanced by lower-tropospheric convergence. From this, (14) indicates that there must be ascent in the right entrance region that is maximized in the middle troposphere. Likewise, convergence in the left entrance region must be balanced by lower-tropospheric divergence; (14) thus indicates that there must be descent in the right entrance region that is maximized in the middle troposphere.

Conversely, as a parcel exits the jet, it moves from west to east at a progressively slower rate of speed, meaning that it decelerates in the eastward (or positive *x*-) direction. Thus, following the flow, the left-hand side of (15a) is negative as *u* decreases. For $f > 0$, v_{ag} is negative, indicating a north-to-south flow across the jet in its exit region. In the absence of ageostrophic flow elsewhere, this implies convergence in the right exit region and divergence in the left exit region. Due to the same principles as in the jet entrance region, this implies middle-tropospheric ascent in the left exit region and middle-tropospheric descent in the right exit region.

We can take these arguments one step further. Assuming weak lower-tropospheric flow and under the constraints of the geostrophic approximation, a westerly jet streak is associated with a westerly thermal wind. A north-south layer-mean temperature gradient with cold air to the north must exist to balance this westerly thermal wind. Thus, the vertical circulation in the jet entrance region is a *direct* circulation, defined as one with ascent in the warm air and descent in the cold air, whereas the vertical circulation in the jet exit region is an *indirect* circulation, defined as one with descent in the warm air and ascent in the cold air.

Surface cyclones tend to develop, or develop most rapidly, when located in the right entrance or left exit regions of an upper-tropospheric jet, where ascent is indicated in Figure 8. We will explore why this is the case in more detail next semester.

The Inclusion of Jet/Flow Curvature

Above, we considered the ageostrophic flow for a "straight" jet streak. However, jet streaks and the synoptic-scale flow accompanying them often exhibit at least weak curvature. An example of a weakly curved jet streak is depicted in Figure 9.

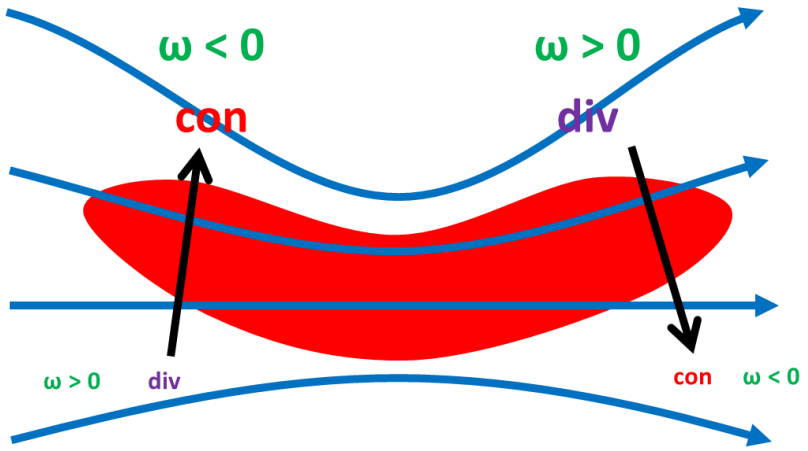

Figure 9. As in Figure 8, except for a curved (along the streamlines) upper tropospheric jet streak. The relative size of the text on each side of the jet indicates the relative magnitudes of divergence and omega on each side of the jet.

The addition of flow curvature contributes another source of ageostrophic flow, that due to curved flow, to that associated with straight-line flow accelerations. In the example in Figure 9, the flow has greater curvature (and thus greater ageostrophic flow) on the left side of the jet, whereas it has weaker curvature (and thus weaker ageostrophic flow) on the right side of the jet. Consequently, convergence/divergence and vertical motion are maximized on the left side of the jet in this case.

The Four-Quadrant Jet Model Applied to Low-Level Jets

Let us consider the four-quadrant jet model applied to low-level jets. For ease of interpretation, let us consider a southerly low-level jet, as depicted in Figure 10, though the basic interpretation can be applied to any low-level jet. From (15b), the ageostrophic wind must be negative (east-to-west) in this low-level jet's entrance region and positive (west-to-east) in this low-level jet's exit region.

From Dines' compensation principle, lower-tropospheric convergence must be balanced by upper-tropospheric divergence, such that (14) indicates that there must be ascent maximized in the middle troposphere in the jet regions with lower-tropospheric convergence. Likewise, lower-tropospheric divergence must be balanced by upper-tropospheric convergence, with (14) indicating descent that is maximized in the middle tropospheric in the jet regions with lower-tropospheric divergence.

Thus, the pattern of ascent and descent is flipped from that with upper-tropospheric jets: ascent is favored in the left entrance and right exit regions and descent is favored in the right entrance and left exit regions.

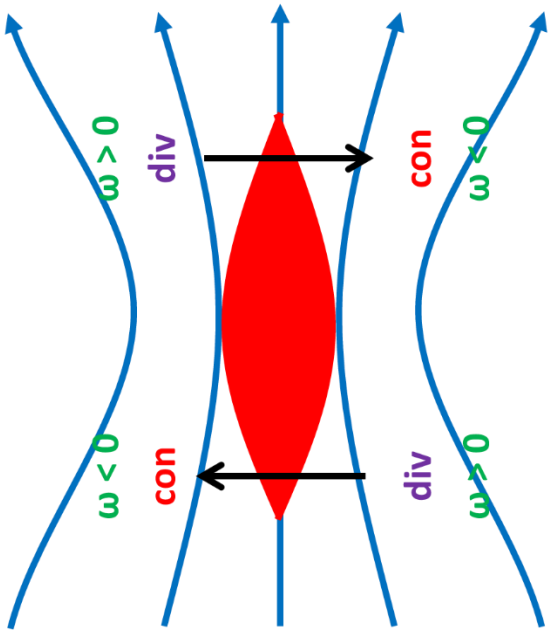

Figure 10. As in Figure 8, except for a low-level jet. Note that the only change between Figures 8 and 10, apart from the direction of the jet, is the sign of omega in each quadrant.